ACS chemical biology

ARTICLES

pubs.acs.org/acschemicalbiology

Evolution of Group 14 Rhodamines as Platforms for Near-Infrared Fluorescence Probes Utilizing Photoinduced Electron Transfer

Yuichiro Koide,[†,‡] Yasuteru Urano,[†] Kenjiro Hanaoka,[†,‡] Takuya Terai,[†,‡] and Tetsuo Nagano[†,‡,*]

[†]Graduate School of Pharmaceutical Sciences, The University of Tokyo, 7-3-1, Hongo, Bunkyo-ku, Tokyo 113-0033, Japan

[‡]CREST, JST, Japan Science and Technology Agency, 3-5 Sanbancho, Chiyoda, Tokyo 102-0075, Japan

Supporting Information

ABSTRACT: The absorption and emission wavelengths of group 14 pyronines and rhodamines, which contain silicon, germanium, or tin at the 10 position of the xanthene chromophore, showed large bathochromic shifts compared to the original rhodamines, owing to stabilization of the LUMO energy levels by $\sigma^*-\pi^*$ conjugation between group 14 atom-C (methyl) σ^* orbitals and a π^* orbital of the fluorophore. These group 14 pyronines and rhodamines retain the advantages of the original rhodamines, including high quantum efficiency in aqueous media (Φ_{fl} = 0.3−0.45), tolerance to photobleaching, and high water solubility. Group 14 rhodamines have higher values of reduction potential than other NIR light-emitting original rhodamines, and therefore, we speculated their NIR fluorescence could be controlled through the photoinduced electron transfer (PeT) mechanism. Indeed, we found that the fluorescence quantum yield (Φ_{fl}) of Si-rhodamine (SiR) and Ge-rhodamine (GeR) could be made nearly equal to zero, and the threshold level for fluorescence on/off switching lies at around 1.3−1.5 V for the SiRs. This is about 0.1 V lower than in the case of TokyoGreens, in which the fluorophore is well established to be effective for PeT-based probes. That is to say, the fluorescence of SiR and GeR can be drastically activated by more than 100-fold through a PeT strategy. To confirm the validity of this strategy for developing NIR fluorescence probes, we employed this approach to design two kinds of novel fluorescence probes emitting in the far-red to NIR region, *i.e.*, a series of pH-sensors for use in acidic environments and a Zn^{2+} sensor. We synthesized these probes and confirmed that they work well.

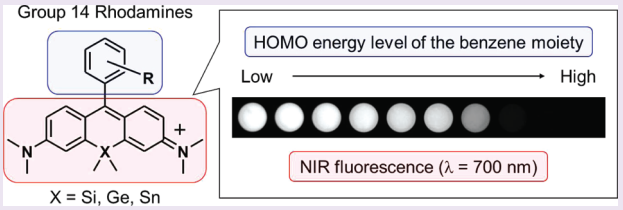

There has been a renaissance period for fluorescence probes in the past few decades. Since the early fluorescent indicators for calcium ion were reported by Tsien in the early 1980s,[1,2] an enormous range of fluorescence molecular probes has been developed and many of them are now commercially available.[3] They include probes for pH[4,5] or environmental changes,[6] metal ions,[7−10] enzymatic activities,[11,12] reactive oxygen and nitrogen species (ROS and RNS),[13−15] and many other analytes. However, most of the probes have their absorption and emission peaks in the UV to visible region (350−600 nm), and the number of fluorescence probes excitable in the far-red or still longer-wavelength near-infrared (NIR) region (>600 nm) is quite small. Nevertheless, the latter probes are of great interest,[16] not only because of their possible application for *in vivo* imaging, but also because they have various attractive features for biological applications, including low background autofluorescence from serum, proteins, and other biological macromolecules, and little risk of cell damage by the excitation light. In other words, dyes that can be excited in the far-red to NIR region are especially suitable as fluorescence probes for use in biological systems.

One reason why not many probes have been reported is that there is only a small number of far-red to NIR-excitable fluorophores that can be used in aqueous media and whose structures can be easily modified. Indeed, the only widely used fluorophore excitable in the long-wavelength region is that of cyanine dyes, *e.g.*, Cy5 and Cy7, which have become widely used as fluorescent labels in clinical and biological chemistry.[17,18] Even so, it is difficult to effectively regulate the fluorescence of cyanine dyes. Resonance energy transfer (RET) is one method to control far-red to NIR fluorescence and has been applied to cyanine dyes.[19,20] However, fluorophores which absorb light in the far-red to NIR region often have long π conjugate systems, so that their structures are relatively large. Since the RET acceptor must absorb at longer wavelength than the fluorophore, the molecular size of the resulting probe becomes extremely large, restricting the flexibility of design and application.

Photoinduced electron transfer (PeT) is one of the most effective methods to control the fluorescence behavior of probes.[12,21] PeT is a well-known mechanism through which the fluorescence of a fluorophore is quenched by electron transfer from the donor to the acceptor moiety. The free energy change of the electron transfer reaction (ΔG_{PeT}) can be estimated by means of the Rehm−Weller equation,[22] $\Delta G_{PeT} = E(D^+/D) - E(A/A^-) - \Delta E_{00} - C$, where ΔE_{00} is the energy of

Received: August 4, 2010
Accepted: March 4, 2011
Published: March 04, 2011

Scheme 1. Synthetic Scheme of Group 14 Pyronines and Rhodamines[a]

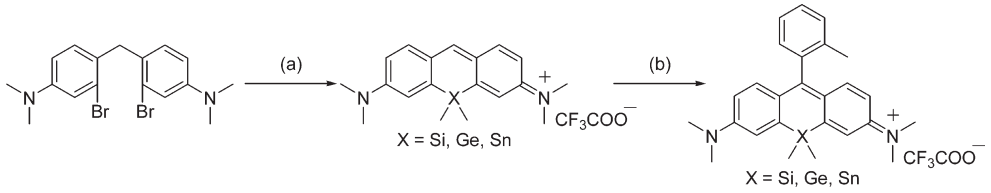

[a] Reagents: (a) (i) *s*-BuLi/THF, −78 °C; (ii) Me_2XCl_2 (X = Si, Ge, Sn)/THF, −78 °C to rt; (iii) chloranil/CH_2Cl_2. (b) (i) 2-MePhLi/THF, −78 °C to rt; (ii) chloranil/CH_2Cl_2. Details are given in Supporting Information.

the zero−zero transition to the lowest excited singlet state of the acceptor fluorophore, upon which the wavelength of the emission depends, $E(D^+/D)$ and $E(A/A^-)$ are the first one-electron oxidation potential of the donor and the first one-electron reduction potential of the acceptor in the solvent under consideration, and C is the work term for the charge separation state. The Rehm−Weller equation, as well as a large number of practical examples, suggests that PeT is very efficient when the separation between the highest occupied molecular orbital (HOMO) and the lowest unoccupied molecular orbital (LUMO) in the fluorophore is relatively large, that is, when the wavelength of the fluorophore is comparatively short.[12,21] On the other hand, in the case of a far-red to NIR fluorophore, it becomes difficult to produce charge separation as a consequence of PeT before the excited electron relaxes to the ground state with emission of a photon, because of the relatively small excitation energy introduced into the system. In addition, ultrafast radiationless deactivation of the excited state occurs efficiently,[23] resulting in reduced quantum yield and less likelihood of strong signal activation by release from PeT regulation. So, it is challenging to control far-red to NIR fluorescence through a PeT process, which is another reason why there are few long wavelength-excitable probes that exhibit drastic fluorescent activation.[24−26]

Recently, group 14 metalloles, silicon-, germanium-, or tin-containing metallocyclopentadienes, have received renewed attention because of their unusual electronic structure and photophysical characteristics,[27−30] and they have been used as building blocks for the construction of π-conjugated polymers.[31] Their intriguing properties have led to applications in a variety of optoelectronic devices, including electron transport materials and organic light-emitting diodes (OLEDs).[32] The key to the extraordinary electronic and optical behavior of group 14 metalloles is their relatively low-lying LUMO levels, owing to $\sigma^*-\pi^*$ conjugation resulting from interaction of the σ^* orbital of the two exocyclic bonds on the ring group 14 atom with the π^* system of the butadiene fragment of the molecule, in sharp contrast to the electronic structure of cyclopentadiene itself.[27−30] In the case of application for fluorescent dyes, the reduced LUMO energy results in a bathochromic shift of the excitation and emission wavelengths. Several examples demonstrate this,[32,33] and a single group has reported that the excitation and emission wavelengths were greatly shifted up to >600 nm by introducing a silicon atom into a xanthene.[34] Rhodamine dyes that contain the pyronine structure are widely used as the chromophore of fluorescence probes, organelle markers, and labeling agents *in vitro* and *in vivo* owing to their excellent photophysical properties, which are favorable for biological applications; these include high water solubility, high fluorescence intensity, pH-independent fluorescence, and tolerance to photobleaching.[3] Therefore, long wavelength-emitting rhodamines could be excellent candidates for activatable fluorescence probes.

Although, as the Rehm−Weller equation[22] indicates, a high value of $E(A/A^-)$ is necessary to quench far-red to NIR fluorescence of the fluorophore because of the small value of ΔE_{00}, the decreased LUMO levels caused by introducing group 14 atoms, which raise the value of $E(A/A^-)$, are favorable for regulation of fluorescence through a PeT process. Thus, we thought that rhodamines containing group 14 atoms[35] might be available as a general platform for a wide range of long-wavelength light-emitting fluorescence probes, in which the fluorescence could be controlled by means of PeT mechanisms. In this work, we newly synthesized several group 14 atom-containing pyronines and rhodamines, as well as their derivatives, to validate our hypothesis on the general design of far-red to NIR excitable fluorescence probes through a PeT strategy.

RESULTS AND DISCUSSION

Synthesis and Photophysical Properties of Group 14 Pyronines and Rhodamines. First, we tried to synthesize modified rhodamines by way of pyronines in which the oxygen atom at the 10 position was replaced with group 14 atoms, silicon, germanium, and tin. As shown in Scheme 1, dilithium reagent was generated from bis(2-bromo-4-dimethylaminophenyl)methane by halogen−metal exchange reaction and quenched with the appropriate dialkyl dichloride of silicon, germanium, or tin, and finally oxidation of the fluorophore afforded the corresponding xanthenes, Si-pyronine (SiP), Ge-pyronine (GeP), and Sn-pyronine (SnP). It has been observed that SnP is unstable in air or in DMSO stock solution and slowly decomposes to generate mainly the corresponding xanthone. Next, we attempted to synthesize the corresponding rhodamines by insertion of 2-methyl phenyl lithium at the 9 position of the xanthenes; this site should be susceptible to nucleophilic attack because of its relative electron deficiency, following oxidation of the fluorophore. Si-rhodamine (SiR) and Ge-rhodamine (GeR) were obtained as stable products. However, although the mass spectrum of Sn-rhodamine (SnR) was clearly detected, this compound decomposed immediately after quenching of the reaction, chiefly affording a malachite green-like compound, presumably *via* an acid-catalyzed ring-opening reaction.[30] Rhodamine is more suitable for biological application than pyronine because of its stability to nucleophiles or a basic environment; the phenyl substituents at the center of the chromophoric system are expected to hinder addition of nucleophiles, including hydroxide anion, and thus to reduce the tendency for decolorization derived from the divided π-electron system.[36] Although insertion of these benzene moieties increases the likelihood of radiationless

dx.doi.org/10.1021/cb1002416 |*ACS Chem. Biol.* 2011, 6, 600–608

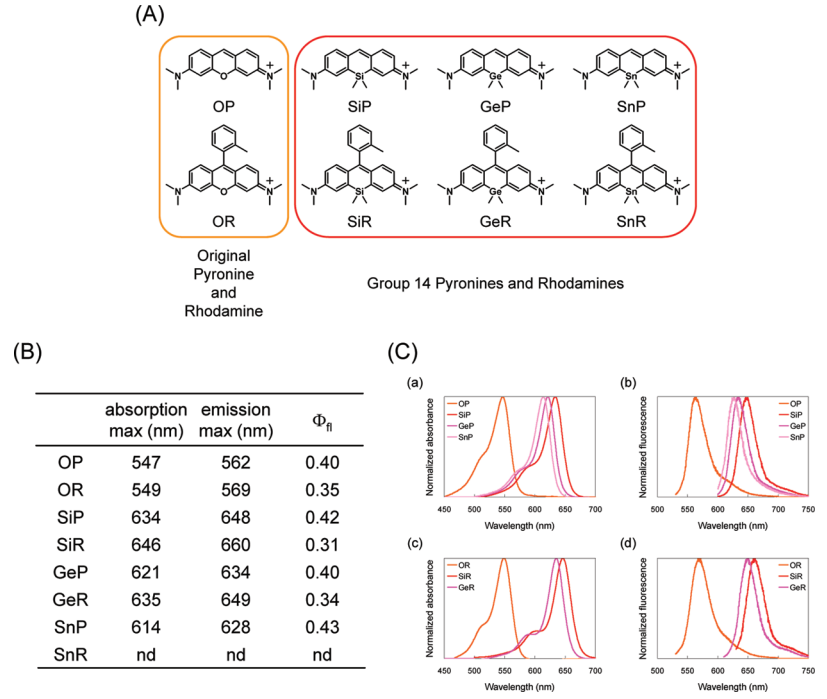

	absorption max (nm)	emission max (nm)	Φ_{fl}
OP	547	562	0.40
OR	549	569	0.35
SiP	634	648	0.42
SiR	646	660	0.31
GeP	621	634	0.40
GeR	635	649	0.34
SnP	614	628	0.43
SnR	nd	nd	nd

Figure 1. Group 14 pyronines and rhodamines. (A) Structures of original and group 14 pyronines and rhodamines. (B) Photophysical properties of original and group 14 pyronines and rhodamines, measured in PBS at pH 7.4. For determination of the fluorescence quantum yield (Φ_{fl}), cresyl violet in MeOH ($\Phi_{fl} = 0.54$) was used as a fluorescence standard. nd = not determinable. (C) Normalized absorption and emission spectra of group 14 pyronines (a, b) and rhodamines (c, d) in PBS at pH 7.4. Spectra of OP and OR are also shown.

energy loss that would reduce the quantum efficiency, the maintenance of an orthogonal relationship between the benzene moiety and the fluorophore by introducing a stopper, the 2-Me group in this case, should reduce the energy loss by restricting rotation.[12] In addition, substitution by aromatic residues tends to cause a slight red shift of absorption and emission. This can be traced to the weak electron-withdrawing effect of such aromatic substituents, which for steric reasons tend to be oriented perpendicular to the chromophoric π-electron system of the dye. Group 14 pyronines and rhodamines showed water solubility similar to that of the original pyronines and rhodamines in the range of practical use ($\sim$1 μM) (Supporting Figure S1). All measurements of absorption and fluorescence were conducted in the presence of 0.1% DMSO as a co-solvent, which was confirmed to be an appropriate concentration.

Figure 1 shows the photophysical properties of the synthesized group 14 pyronines and rhodamines, as well as the classic O-pyronine (OP) and O-rhodamine (OR), in aqueous media. Although in general the fluorescence quantum yield of a dye becomes smaller as the wavelength become longer and most dyes whose wavelength is around 650 nm have a quantum yield smaller than 0.3 in aqueous solution,[37,38] all of the prepared fluorophores were highly fluorescent, with $\Phi_{fl} = 0.3-0.45$, which is close to those of OP and OR. In addition, their absorption and emission bands were similarly shaped and greatly red-shifted to the far-red to NIR region, depending on the identity of the group 14 element. Interestingly, the extent of red shift did not correlate with the atom size in the case of group 14 pyronines and rhodamines (C < Sn < Ge < Si),[35] unlike group 16 pyronines and rhodamines (O < S < Se < Te).[39,40] This observation can be attributed to the difference in the mechanism of the bathochromic shift. For group 14, as described above, the LUMO of the π-system is stabilized by $\sigma^*-\pi^*$ conjugation between the group 14 atom-C (methyl) σ^* orbital and a π^* orbital of the fluorophore, except for the case of C-pyronines and C-rhodamines, and the orbital interaction between the carbon π^* and the σ^* of the group 14 element becomes less efficient as the latter becomes larger, because the group 14 atom-C (π-system) distance increases.[29,30] In the case of C-pyronines and C-rhodamines, the $\sigma^*-\pi^*$ conjugation is almost negligible, as in cyclopentadiene.[27] On the other hand, for group 16, the red shift is thought to be due to the resonance effect of the chalcogen atom, which delocalizes the positive charge in the fluorophore and consequently decreases the HOMO−LUMO gap.[39,40] This resonance effect also decreases the quantum yield of group 16 rhodamines as the atomic number increases, through the heavy atom effect, which is another point of difference from group 14 pyronines and rhodamines.

Fluorescence Regulation through PeT Process and Determination of On/Off Threshold of SiRs. To investigate the feasibility of fluorescence regulation of group 14 rhodamines through a PeT strategy, we first measured their reduction potential by cyclic voltammetry. For comparison, the reduction potentials of fluorescein, in which the fluorescence is already known to be highly regulated by PeT; rhodamine B, one of original rhodamines, which absorbs visible light; and IC5, 1,1′,3,3,3′,3′-hexamethylindodicarbocyanine, which absorbs light in the far-red region, were also acquired (Figure 2A). When we used the value of $-E(A/A^-) - \Delta E_{00}$ as an index for occurrence of electron transfer, we found that SiR and GeR showed similar values; that of SiR was lower than those of fluorescein and IC5 by 0.13 and 0.24 V, respectively, and similar to that of visible light-emitting rhodamine B. Thus, fluorescence of SiR and GeR should be amenable to control by PeT. As another approach to obtain

dx.doi.org/10.1021/cb1002416 |ACS Chem. Biol. 2011, 6, 600–608

(A)

	ΔE_{00} eV	$E(A/A^-)$ V (vs SCE)	$-E(A/A^-)-\Delta E_{00}$
SiR	1.90	−0.62	−1.28
GeR	1.93	−0.64	−1.29
Fluorescein	2.43	−1.28	−1.15
Rhodamine B	2.20	−0.75	−1.25
IC5	1.92	−0.88	−1.04

(B)

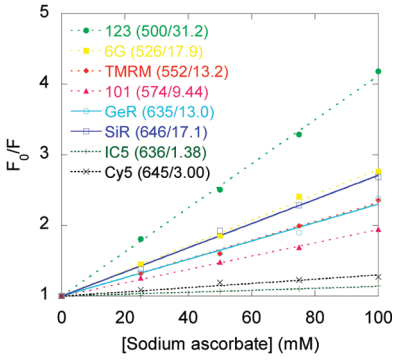

(C)

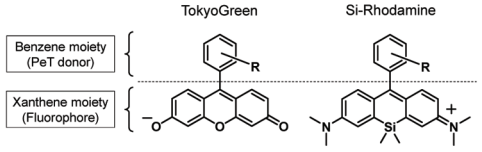

(D)

Entry	R	absorption max (nm)	emission max (nm)	oxidation potential (V vs SCE)	HOMO energy (hartrees)	Φ_{fl}
1	2-Me	646	660	2.19	−0.2356	0.31
2	2,4-DiMe	646	660	2.08	−0.2304	0.32
3	2,5-DiMe	646	660	1.98	−0.2262	0.32
4	2-OMe	649	663	1.75	−0.2174	0.29
5	2-Me-4-OMe	648	662	1.66	−0.2141	0.29
6	2-OMe-5-Me	649	664	1.57	−0.2098	0.28
7	2,4-DiOMe	649	663	1.44	−0.2063	0.20
8	2.5-DiOMe	651	665	1.26	−0.1985	0.025
9	2-Me-4-NMe_2	646	663	0.66	−0.1780	0.001
10	2-Me-5-NMe_2	646	662	0.65	−0.1749	0.001

(E)

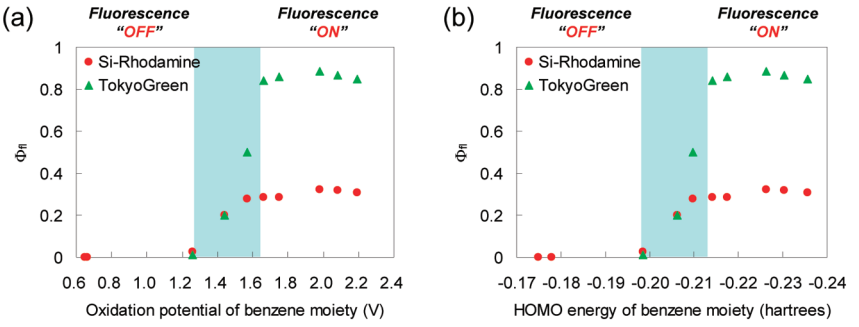

(F)

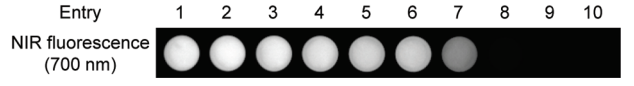

Figure 2. PeT regulation of Si-rhodamines. (A) The values of excitation energy (ΔE_{00}) and reduction potential ($E(A/A^-)$) of SiR, GeR, fluorescein, rhodamine B, and IC5 in the Rehm−Weller equation ($\Delta G_{PeT} = E(D^+/D) - E(A/A^-) - \Delta E_{00} - C$). (B) Stern−Volmer plot of various rhodamines and cyanines with sodium L-ascorbate in PBS at pH 7.4. The numbers in parentheses show the dye's absorption maximum wavelength and the quenching constant (K_{sv}). Excitation and detection wavelengths were 490/525 nm for rhodamine 123 (123), 520/550 nm for rhodamine 6G (6G), 550/575 nm for tetramethylrhodamine (TMRM), 580/600 nm for rhodamine 101 (101), 630/650 nm for GeR and IC5, 640/660 nm for SiR and Cy5 Mono-Reactive Dye (GE Healthcare) (Cy5). (C) Structures of TokyoGreen[12] and Si-rhodamine, shown divided into two parts, the benzene moiety and the fluorophore. (D) Photophysical properties of Si-rhodamines, measured in PBS at pH 7.4, and oxidation potentials and HOMO energy levels of the corresponding benzene moieties. For determination of the quantum efficiency of fluorescence (Φ_{fl}), cresyl violet in MeOH ($\Phi_{fl} = 0.54$) was used as a fluorescence standard. (E) Relationships between the oxidation potential (a) and HOMO energy (b) of the benzene moiety and the Φ_{fl} of Si-rhodamine and TokyoGreen. (F) NIR fluorescence (700 nm) images of Si-rhodamines at equimolar concentration. Entry numbers correspond to those in panel D.

further confirmation, we conducted a Stern−Volmer quenching experiment of SiR and GeR with sodium L-ascorbate as an electron donor to evaluate how easily their fluorescence is quenched through the PeT process in comparison with that of visible-emitting original rhodamines and cyanine dyes, which have wavelengths similar to those of SiR and GeR (Figure 2B). The results clearly show that it becomes more difficult to control the fluorescence of original rhodamines as their wavelengths become longer (that is, if the dye were a NIR light-emitting original O-rhodamine, it would be much more difficult to highly

dx.doi.org/10.1021/cb1002416 |ACS Chem. Biol. 2011, 6, 600–608

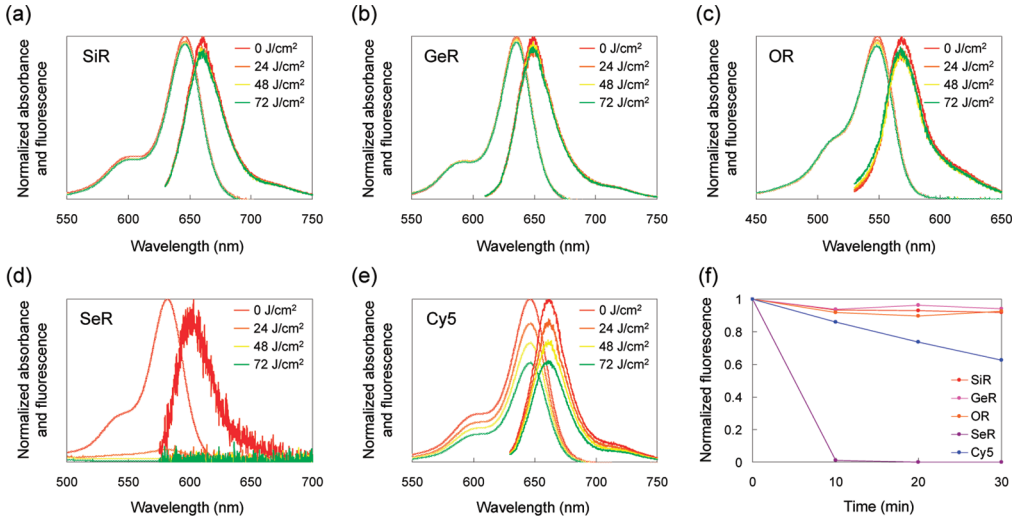

Figure 3. Photobleaching test. Normalized absorption and emission spectra (a−e) and fluorescence changes (f) of 1 μM 2-Me SiR, 2-Me GeR, 2-Me OR, 2-Me SeR, and Cy5 in PBS at pH 7.4 were measured during light illumination. Samples were exposed to light (40 mW/cm^2) for 0, 10, 20, or 30 min.

regulate its fluorescence). Further, SiR and GeR have almost the same quenching constants as rhodamine 6G (17.9) and tetramethylrhodamine (13.2), respectively, which have wavelengths as much as 100 nm shorter than those of SiR (17.1) and GeR (13.0), unlike the cyanine dyes, IC5 (1.38) and Cy5 (3.00), which show much smaller quenching constants. These experimental data also support the validity of our hypothesis that fluorescence probes operating in the red to NIR region could be developed by using group 14 rhodamines in the same way that many kinds of fluorescence probes have been obtained based on visible light-excitable fluorophores (such as the original rhodamines) and the PeT strategy.

With these results in hand, we synthesized 10 SiR derivatives by one-step synthesis from Si-Xanthone to examine in detail the utility of group 14 rhodamines as a fluorophore for PeT-based probes by comparing the ease of regulation of their fluorescence by PeT with that of TokyoGreens,[12] in which the fluorophore is well established to be effective for PeT-based probes. The SiR derivatives have various HOMO energy levels of the benzene moiety; the HOMO energy level could be finely tuned by introducing methyl, methoxy, and dimethylamine groups into the benzene moiety. As with TokyoGreens, the fact that the absorption and emission maxima were not altered among SiR derivatives shows that ground-state interaction between the benzene moiety and the xanthene chromophore is minimal in all of them. On the other hand, the fluorescence quantum yield was greatly altered, depending on the oxidation potential and the HOMO energy level of the benzene moiety. In the case of SiR derivatives whose oxidation potential of the benzene moiety is higher than 1.6 V (vs SCE), high Φ_{fl} values were observed in aqueous media at pH 7.4. Below 1.6 V, the Φ_{fl} values dropped sharply with decreasing oxidation potential and finally reached almost zero (Φ_{fl} = 0.001) in the case where the benzene moiety was *m*- or *p*-dimethylaminotoluene, whose oxidation potentials are 0.66 and 0.65 V, respectively (Figure 2D, E). For Cy7, in contrast, Φ_{fl} does not approach zero even in the case of *o*-diaminobenzene, which has a much lower oxidation potential.[24] From these results, the threshold level for on/off switching of fluorescence lies at around 1.3−1.5 V for the SiRs, which is about 0.1 V lower than that of TokyoGreens. Similarly, a GeR derivative containing *m*-dimethylaminotoluene was synthesized, and its photophysical properties were examined. We found that its quantum yield was also highly regulated by a PeT process (Φ_{fl} = 0.001). Consequently, SiR- and GeR-based probes could achieve high fluorescence activation *via* a PeT strategy.

Photostability of SiR and GeR. For a satisfactory signal-to-background ratio, it is crucial to choose a dye with good fluorescence properties. The suitability of a dye is determined by its fluorescence and triplet quantum yield, molar absorption coefficient, wavelengths of absorption and emission, tolerance to photobleaching, and water-solubility, as well as other considerations. Among these properties, the photostability is of major importance for fluorescent probes, because photodegradation leads to irreversible loss of fluorescence.

We investigated whether SiR and GeR are as tolerant to photobleaching as classic rhodamines, which have excellent photostability.[41,42] Figure 3 shows the change of the absorption and emission spectra of 2-Me SiR and 2-Me GeR, as representatives of SiRs and GeRs, upon light irradiation. 2-Me OR, which is a representative of classic rhodamines; 2-Me SeR,[39,40] which is one of the group 16 rhodamines; and Cy5, which absorbs light in the same color region and is widely used as a labeling agent for biomolecules, were also examined for comparison. Unlike SeR or Cy5, which showed extensive degradation, little diminution of absorption or emission was detected in the cases of SiR, GeR, and OR. Although small structural change sometimes induces a big difference in properties and SeR is not photostable, SiR and GeR have excellent tolerance to photobleaching, like traditional rhodamines.

pH-Dependent Fluorescence Change of SiR and GeR Containing an Aniline Moiety. As mentioned above, *m*- and *p*-dimethylaminotoluene have sufficiently high HOMO energy levels to cause PeT toward the SiR or GeR fluorophore, and in an aqueous solution at acidic pH, their fluorescence intensity was increased. We can explain this recovery of the fluorescence under acidic conditions in terms of amino group protonation, which reduces the electron-donating ability of the aminobenzene moiety and abolishes the PeT. Since the value of pK_a depends on the substitution of the *N*-alkyl group of the aniline moiety, it should be possible to develop a series of fluorescent compounds

dx.doi.org/10.1021/cb1002416 |*ACS Chem. Biol.* 2011, 6, 600–608

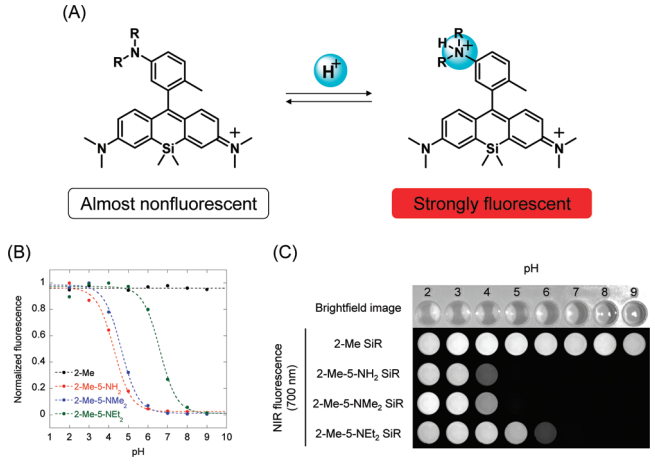

Figure 4. NIR fluorescence-emitting pH-sensors for acidic environment. (A) A scheme for the reversible and acidic pH-induced fluorescence activation of a probe. (B) pH-dependent changes in emission intensity of 2-Me-5-NH_2 SiR (pK_a = 4.3), 2-Me-5-NMe_2 SiR (pK_a = 4.6), and 2-Me-5-NEt_2 SiR (pK_a = 6.6), as acidic pH-sensitive fluorescence probes and 2-Me SiR as a control always-on probe. Curve fitting was based on a modified Henderson−Hasselbach equation. (C) pH profiles of fluorescence of acidic pH-activatable SiR probes.

with a range of pK_a values. On the basis of this strategy, we developed a series of novel, acidic pH-sensitive fluorescence probes bearing various aniline structures as the benzene moiety. All these compounds were almost nonfluorescent in nonprotonated form, owing to PeT from the aniline moiety to the fluorophore, but became highly fluorescent in the protonated form, showing a greater than 100-fold activation of fluorescence.

Figure 4 shows the pH-dependent changes in emission intensity of these pH-sensitive SiRs, as well as the constant emission from pH-independent 2-Me SiR. The compounds work as pH-sensors that have different pK_a values, depending on the alkyl group on the nitrogen. Acidity-sensing fluorescent probes have been used in many ways to elucidate a variety of cellular events that are influenced by intracellular pH, including endocytosis, phagocytosis, enzymatic activity, ion transport, and homeostasis.[43,44] As an advanced application of fluorescent probes sensing an acidic environment, selective molecular imaging of viable cancer cells was recently achieved.[5] To our knowledge, there has been no pK_a-tunable pH-sensor based on a NIR light-emitting fluorophore, so our SiR-based pH-sensors are likely to find many applications *in vitro* and *in vivo*.

Application of SiR and GeR to Living Cells. We applied 2-Me SiR and 2-Me GeR to living HeLa cells to elucidate whether they could be easily loaded into cells across the cell membrane without modification, like the original rhodamines. The original rhodamines are mostly localized in mitochondria in living cells because of their cationic and lipophilic character, and several rhodamines, such as rhodamine 123 and tetramethylrhodamine, are widely used as stains for mitochondria.[3,45] Simultaneously, to assess the localization of SiR and GeR in living cells, the HeLa cells were costained with mitotracker green FM. Fluorescence images of 2-Me SiR and 2-Me GeR were both well merged with that of mitotracker green FM; specifically, SiR and GeR are preferentially localized in mitochondria (Figure 5). Since SiR and GeR have high reduction potential, it is possible that they might be reduced in living cells, the internal environment of which is known to be normally reductive; however, in fact, they emitted

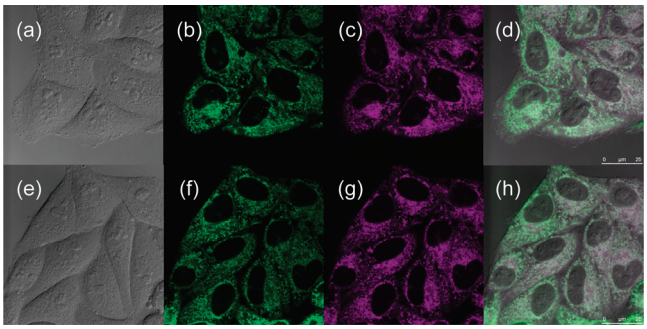

Figure 5. Localization of 2-Me SiR (a−d) and 2-Me GeR (e−h) in mitochondria in HeLa cells. 2-Me SiR or 2-Me GeR (1 μM) and MitoTracker Green FM (500 nM) were loaded into HeLa cells for 30 min. (a, e) Brightfield image. (b, f) Fluorescence image of MitoTracker Green FM. (c, g) Fluorescence image of 2-Me SiR or 2-Me GeR. (d, h) Merged image.

bright fluorescence in the cells without fading, and no indication of toxicity was seen during the observations (data not shown).

Development of Novel NIR Fluorescence Probe for Zinc Ion Based on PeT Strategy. In principle, our findings described earlier allow us to design not only pH-sensors but also many kinds of NIR light-emitting fluorescence probes, on the basis of the change of HOMO energy level of the benzene moiety upon encountering a target molecule. As an example, we were able to develop a novel fluorescence probe for zinc ion (Zn^{2+}), which is a vital component in many cellular processes. Zn^{2+} facilitates essential biological functions and disorder of its metabolism is closely associated with many severe neurological diseases, including Alzheimer's disease, cerebral ischemia, and epilepsy.[46,47] Since the mechanisms by which Zn^{2+} mediates neurotransmission and exerts potent neurotoxic effects are still largely unknown, measurement of Zn^{2+} is important in neurobiology. In recent years, significant advances have been made in the design of fluorescence probes for Zn^{2+} for the investigation of zinc physiology.[9,10] A number of fluorescent Zn^{2+} sensors are commercially available and suitable for biological applications and have been used with some success.[48,49] A few Zn^{2+} sensors with excitation and emission at longer wavelengths than far-red have been also reported.[50] However, by utilizing the PeT strategy, we have newly developed a novel NIR light-emitting Zn^{2+} sensor with desirable properties for biological applications, including high signal amplification, high fluorescence intensity, high water solubility, and tolerance to photobleaching. Sensors with such properties are expected to be particularly suitable for multicolor imaging and for detection at sites deep within samples.

In designing such a NIR light-emitting Zn^{2+} sensor, we focused on the highly activatable green-fluorescent Zn^{2+} probe, ZnAF-2, which our group reported previously.[8] ZnAF-2 contains an alkylaminobenzene moiety, and taking the results shown in Figure 2 into consideration, we thought that this moiety would be able to regulate the fluorescence of SiR through the PeT process. Thus, we synthesized SiR-Zn, which was expected to show fluorescence activation upon capturing free Zn^{2+}.

Figure 6 clearly shows that SiR-Zn operates as a fluorescent sensor for Zn^{2+}. SiR-Zn emits greater fluorescence as the concentration of free Zn^{2+} is increased (~15-fold activation at maximum). The K_d value of SiR-Zn was 1.4 nM, which is similar to that of ZnAF-2 bearing the same chelating moiety, and it

dx.doi.org/10.1021/cb1002416 |*ACS Chem. Biol.* 2011, 6, 600–608

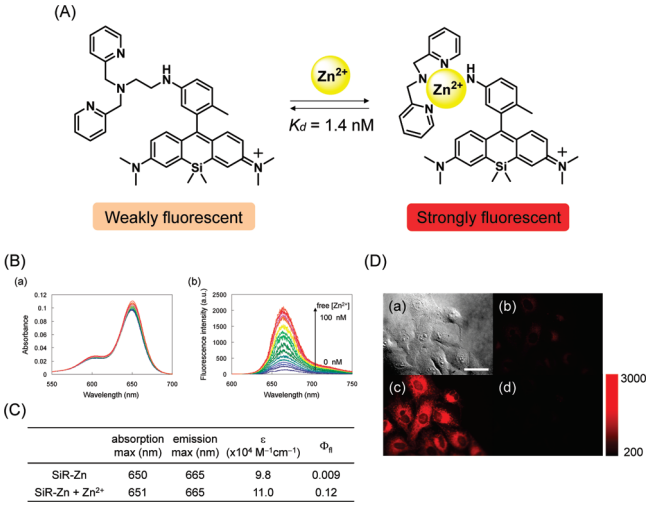

Figure 6. NIR fluorescence-emitting Zn^{2+} sensor. (A) Scheme for reversible Zn^{2+}-induced fluorescence activation of a probe. (B) Absorption (a) and emission (b) spectra of 1 μM SiR-Zn in the presence of various concentrations of free Zn^{2+} (0 to 100 nM free Zn^{2+}) in 100 mM HEPES buffer containing 100 mM $NaNO_3$ and 10 mM NTA at pH 7.4. The excitation wavelength was 650 nm. (C) Photophysical properties of SiR-Zn in the absence and presence of Zn^{2+}, measured in 100 mM HEPES buffer containing 100 mM $NaNO_3$ and 10 mM NTA at pH 7.4. In the presence of Zn^{2+}, the concentration of free Zn^{2+} was 100 nM. For determination of the quantum efficiency of fluorescence (Φ_{fl}), cresyl violet in MeOH (Φ_{fl} = 0.54) was used as a fluorescence standard. (D) Fluorescence imaging of intracellular Zn^{2+} using SiR-Zn. HeLa cells incubated with 1 μM SiR-Zn for 30 min at 37 °C were washed with fresh medium, SiR-Zn-stained cells were exposed to 5 μM pyrithone and 50 μM Zn^{2+} for 5 min, and return of intracellular Zn^{2+} to the resting level was achieved by addition of 100 μM TPEN. (a) Brightfield image. (b) Fluorescence image after loading of SiR-Zn. (c) Fluorescence image of SiR-Zn after addition of pyrithion and Zn^{2+}. (d) Fluorescence image after addition of TPEN. Scale bar represents 50 μm.

should be possible to obtain a range of K_d values by changing the Zn^{2+} chelating moiety in the same way as has been done with ZnAFs. Next, the titration of SiR-Zn with various metal ions was conducted to examine the metal selectivity (Supplementary Figure S5). The fluorescence of SiR-Zn was not influenced by other cations, such as Na^+, K^+, Mg^{2+}, and Ca^{2+}, which exist at high concentrations under physiological conditions, even at as high a concentration as 5 mM. As regards heavy metal cations, we observed fluorescence increases of SiR-Zn with Co^{2+} and Cd^{2+}, other than Zn^{2+}, but Co^{2+} and Cd^{2+} would have little influence *in vivo*, since the free cations exist at very low concentrations.

We next demonstrated the application of SiR-Zn for fluorescence imaging of Zn^{2+} in cultured living cells. SiR-Zn-loaded HeLa cells showed a remarkable fluorescence increase upon addition of Zn^{2+} with 2-mercaptopyridine *N*-oxide (pyrithion), a Zn^{2+} selective ionophore, and subsequent addition of an excess of *N*,*N*,*N*′,*N*′-tetrakis(2-pyridylmethyl)ethylenediamine (TPEN), a strong chelater of Zn^{2+}, resulted in a decrease of the fluorescence to the initial range (Figure 6). These results clearly show not only that SiR-Zn has potential for biological application but also that the combination of SiR and PeT is a versatile design strategy for far-red to NIR emitting fluorescent probes.

Conclusion. In summary, we have synthesized group 14 pyronines and rhodamines in which the oxygen atom at the 10 position is replaced by silicon, germanium, or tin and examined their photophysical properties. All of these group 14 pyronines and rhodamines have high quantum efficiency (Φ_{fl} = 0.3−0.45), unlike group 16 rhodamines. Using 2-Me SiR and 2-Me GeR as representatives of SiRs and GeRs, we showed that SiR and GeR have excellent tolerance to photobleaching, equivalent to that of the original rhodamines, and could be easily loaded into living cells without any need for modification. Intracellularly, they emitted strong fluorescence with little fading. The results of cyclic voltammetry and Stern−Volmer quenching experiments indicated that the far-red to NIR fluorescence of SiR and GeR could be controlled through PeT, so we synthesized a series of SiR derivatives with various HOMO energy levels of the benzene moiety by introducing methyl, methoxy, and dimethylamine groups into the benzene moiety. We found that Φ_{fl} of SiR and GeR could be made nearly equal to zero, and the threshold level for on/off switching of fluorescence lay at around 1.3−1.5 V for the SiRs. This is about 0.1 V lower than in the case of Tokyo-Greens, in which the fluorophore is well established to be suitable for PeT-based probes. That is to say, the fluorescence of SiR and GeR can be activated more than 100-fold *via* a PeT strategy. Therefore, our approach of using a PeT strategy with group 14 rhodamines provides, we believe, a general platform for a wide range of long-wavelength light-emitting fluorescent probes that retain the advantages of rhodamine for biological applications, especially as regards tolerance to photobleaching. To confirm and demonstrate the validity of the design strategy, we developed two kinds of novel NIR light-emitting fluorescence probes, *i.e.*, a series of pH-sensors for use in acidic environments and a Zn^{2+} sensor.

METHODS

General Methods. General chemicals were of the best grade available, supplied by Tokyo Chemical Industries, Wako Pure Chemical, Aldrich Chemical Co., Alfa Aesar, Dojindo, GE Healthcare, and Invitrogen, and were used without further purification. All solvents were used after appropriate distillation or purification. NMR spectra were recorded on a JEOL JNM-LA300 instrument at 300 MHz for ^{1}H NMR and at 75 MHz for ^{13}C NMR or a JEOL JNM-LA400 instrument at 400 MHz for ^{1}H NMR and at 100 MHz for ^{13}C NMR. Mass spectra (MS) were measured with a JEOL JMS-T100LC AccuToF using ESI, and δ values are given in ppm relative to tetramethylsilane. HPLC analysis was performed on an Inertsil ODS-3 (4.6 × 250 mm) column (GL Sciences Inc.) using an HPLC system composed of a pump (PU-980, JASCO) and a detector (MD-2015 or FP-2025, JASCO). Preparative HPLC was performed on an Inertsil ODS-3 (10.0 × 250 mm) column (GL Sciences Inc.) using an HPLC system composed of a pump (PU-2080, JASCO) and a detector (MD-2015 or FP-2025, JASCO).

Chemical Synthesis. For details of synthetic procedures and characterization of products, see Supporting Information.

UV−vis Absorption and Fluorescence Spectroscopy. UV−vis spectra were obtained on a Shimadzu UV-1650. Fluorescence spectroscopic studies were performed on a Hitachi F4500. The slit width was 2.5 nm for both excitation and emission. The photomultiplier voltage was 700 V. Relative fluorescence quantum efficiency of group 14 pyronines and rhodamines was obtained by comparing the area under the emission spectrum of the test sample excited at 600 nm with that of a solution of cresyl violet in MeOH, which has a quantum efficiency of 0.54, and those of original xanthene and rhodamine were referred to Rhodamine B in EtOH, whose quantum efficiency is 0.68. In photobleaching tests, samples were exposed to light from a xenon lamp (AH2-RX; Olympus), which was passed through a Cy5 filter (BP630-650;

Olympus) for SiR, GeR, and Cy5; a U-MNG2 filter (BP530-550; Olympus) for OR; or a U-MWYI2 filter (BP545-580; Olympus) for SeR. The excitation and detection wavelengths were 620 and 660 nm for SiR and Cy5, 600 and 650 nm for GeR, 525 and 570 nm for OR, and 570 and 600 nm for SeR, respectively.

Cyclic Voltammetry. Cyclic voltammetry was performed on a 600A electrochemical analyzer (ALS). A three-electrode arrangement in a single cell was used for the measurements: a Pt wire as auxiliary electrode, a glassy carbon electrode as the working electrode, and a Ag/Ag^+ electrode as the reference electrode. The sample solutions contained a sample and 100 mM tetrabutylammonium perchlorate (TBAP) as a supporting electrolyte in acetonitrile, and argon was bubbled for 10 min before measurement. Obtained potentials (vs Ag/Ag^+) were converted to those vs SCE by adding 0.248 V.

Calculation. HOMO energy levels were calculated at the B3LYP/6-31G level with Gaussian 98W.

Fluorescence Imaging of 96-Well Plates. Fluorescence images of 96-well plates were captured with a Maestro In-Vivo Imaging System (CRI Inc., Woburn, MA). The excitation wavelength was 590−650 nm, and the detection fluorescence wavelength was 700 nm.

Fluorescence Imaging of Distribution of SiR and GeR. A confocal imaging system (TCS-SP5; Leica) equipped with an argon laser and a white light laser was used. Fluorescence images were taken with simultaneous monitoring of fluorescence at two channels (WL1 = 500−530 nm, WL2 = 650−700 nm). Excitation wavelengths of 488 nm (argon laser) and 633 nm (white light laser) were used. HeLa cells were cultured in Dulbecco's modified Eagle's medium (DMEM) (Invitrogen Corp.) supplemented with 10% (v/v) fetal bovine serum (Invitrogen Corp.), 1% penicillin, and 1% streptomycin (Invitrogen Corp.) in a humidified incubator containing 5% CO_2 in air. For fluorescence microscopy, HeLa cells were plated in a 35-mm PDL-coated glass-bottomed dish (MatTek Corporation) in Dulbecco's modified Eagle's medium (DMEM).

Fluorescence Imaging of SiR-Zn. The imaging system comprised an inverted microscope (IX 71; Olympus) and cooled CCD camera (Cool Snap HQ; Roper Scientific, Tucson, AZ). The microscope was equipped with a xenon lamp (AH2-RX; Olympus), a 40X objective lens (Uapo/340, N. A. 1.35; Olympus), and a fluorescence mirror unit (U-DM-CY5, Olympus). The whole system was controlled with MetaFluor 6.1 software (Universal Imaging, Media, PA). HeLa cells were cultured in Dulbecco's modified Eagle's medium (DMEM) (Invitrogen Corp.) supplemented with 10% (v/v) fetal bovine serum (Invitrogen Corp.), 1% penicillin, and 1% streptomycin (Invitrogen Corp.) in a humidified incubator containing 5% CO_2 in air. For fluorescence microscopy, HeLa cells were plated in a 35-mm PDL-coated glass-bottomed dish (MatTek Corporation) in Hanks' balanced salt solution (HBSS).

■ ASSOCIATED CONTENT

Supporting Information. Synthesis, HPLC charts, experimental details, and characterization of group 14 pyronines and rhodamines. This material is available free of charge *via* the Internet at http://pubs.acs.org.

■ AUTHOR INFORMATION

Corresponding Author

*Tel: +81-3-5841-4850. Fax: +81-3-5841-4855. E-mail: tlong@mol.f.u-tokyo.ac.jp.

■ ACKNOWLEDGMENT

This study was supported in part by a research grant from New Energy and Industrial Technology Development Organization (NEDO), and by research grants (Grant Nos. 20117003, and 19205021 to Y.U.) from the Ministry of Education, Culture, Sports, Science and Technology of the Japanese Government, and a grant from the Kato Memorial Bioscience Foundation to Y.U.

■ REFERENCES

(1) Grynkiewicz, G., Poenie, M., and Tsien, R. Y. (1985) A new generation of Ca^{2+} indicators with greatly improved fluorescence properties. *J. Biol. Chem. 260*, 3440–3450.

(2) Tsien, R. Y. (1980) New calcium indicators and buffers with high selectivity against magnesium and protons: design, synthesis, and properties of prototype structures. *Biochemistry 19*, 2396–2404.

(3) Haugland, R. P., Ed. (2005) *The Handbook, A Guide to Fluorescent Probes and Labeling Technologies*, 10th ed., Molecular Probes, Inc.: Eugene, OR.

(4) Salerno, M., Ajimo, J. J., Dudley, J. A., Binzel, K., and Urayama, P. (2007) Characterization of dual-wavelength seminaphthofluorescein and seminapthorhodafluor dyes for pH sensing under high hydrostatic pressures. *Anal. Biochem. 362*, 258–67.

(5) Urano, Y., Asanuma, D., Hama, Y., Koyama, Y., Barrett, T., Kamiya, M., Nagano, T., Watanabe, T., Hasegawa, A., Choyke, P. L., and Kobayashi, H. (2009) Selective molecular imaging of viable cancer cells with pH-activatable fluorescence probes. *Nat. Med. 15*, 104–109.

(6) Sunahara, H., Urano, Y., Kojima, H., and Nagano, T. (2007) Design and synthesis of a library of BODIPY-based environmental polarity sensors utilizing photoinduced electron-transfer-controlled fluorescence ON/OFF switching. *J. Am. Chem. Soc. 129*, 5597–5604.

(7) Nolan, E. M., and Lippard, S. J. (2008) Tools and tactics for the optical detection of mercuric ion. *Chem. Rev. 108*, 3443–3480.

(8) Hirano, T., Kikuchi, K., Urano, Y., and Nagano, T. (2002) Improvement and biological applications of fluorescent probes for zinc, ZnAFs. *J. Am. Chem. Soc. 124*, 6555–6562.

(9) Kikuchi, K., Komatsu, K., and Nagano, T. (2004) Zinc sensing for cellular application. *Curr. Opin. Chem. Biol. 8*, 182–191.

(10) Nolan, E. M., and Lippard, S. J. (2009) Small-molecule fluorescent sensors for investigating zinc metalloneurochemistry. *Acc. Chem. Res. 42*, 193–203.

(11) Fujikawa, Y., Urano, Y., Komatsu, T., Hanaoka, K., Kojima, H., Terai, T., Inoue, H., and Nagano, T. (2008) Design and synthesis of highly sensitive fluorogenic substrates for glutathione S-transferase and application for activity imaging in living cells. *J. Am. Chem. Soc. 130*, 14533–14543.

(12) Urano, Y., Kamiya, M., Kanda, K., Ueno, T., Hirose, K., and Nagano, T. (2005) Evolution of fluorescein as a platform for finely tunable fluorescence probes. *J. Am. Chem. Soc. 127*, 4888–4894.

(13) Koide, Y., Urano, Y., Kenmoku, S., Kojima, H., and Nagano, T. (2007) Design and synthesis of fluorescent probes for selective detection of highly reactive oxygen species in mitochondria of living cells. *J. Am. Chem. Soc. 129*, 10324–10325.

(14) Kenmoku, S., Urano, Y., Kojima, H., and Nagano, T. (2007) Development of a highly specific rhodamine-based fluorescence probe for hypochlorous acid and its application to real-time imaging of phagocytosis. *J. Am. Chem. Soc. 129*, 7313–7318.

(15) Kojima, H., Nakatsubo, N., Kikuchi, K., Kawahara, S., Kirino, Y., Nagoshi, H., Hirata, Y., and Nagano, T. (1998) Detection and imaging of nitric oxide with novel fluorescent indicators: diaminofluoresceins. *Anal. Chem. 70*, 2446–2453.

(16) Weissleder, R. (2001) A clearer vision for in vivo imaging. *Nat. Biotechnol. 19*, 316–317.

(17) Ogawa, M., Kosaka, N., Choyke, P. L., and Kobayashi, H. (2009) In vivo molecular imaging of cancer with a quenching near-infrared fluorescent probe using conjugates of monoclonal antibodies and indocyanine green. *Cancer Res. 69*, 1268–1272.

(18) Medarova, Z., Rashkovetsky, L., Pantazopoulos, P., and Moore, A. (2009) Multiparametric monitoring of tumor response to chemotherapy by noninvasive imaging. *Cancer Res. 69*, 1182–1189.

(19) Xing, B., Khanamiryan, A., and Rao, J. (2005) Cell-permeable near-infrared fluorogenic substrates for imaging beta-lactamase activity. *J. Am. Chem. Soc. 127*, 4158–4159.

(20) Blum, G., von Degenfeld, G., Merchant, M. J., Blau, H. M., and Bogyo, M. (2007) Noninvasive optical imaging of cysteine protease activity using fluorescently quenched activity-based probes. *Nat. Chem. Biol. 3*, 668–677.

(21) de Silva, A. P., Gunaratne, H. Q., Gunnlaugsson, T., Huxley, A. J. M., McCoy, C. P., Rademacher, J. T., and Rice, T. E. (1997) Signaling recognition events with fluorescent sensors and switches. *Chem. Rev. 97*, 1515–1566.

(22) Rehm, D., and Weller, A. (1970) Kinetics of fluorescence quenching by electron and H-atom transfer. *Isr. J. Chem. 8*, 259–271.

(23) Sanchez-Galvez, A., Hunt, P., Robb, M. A., Olivucci, M., Vreven, T., and Schlegel, H. B. (2000) Ultrafast radiationless deactivation of organic dyes: evidence for a two-state two-mode pathway in polymethine cyanines. *J. Am. Chem. Soc. 122*, 2911–2924.

(24) Sasaki, E., Kojima, H., Nishimatsu, H., Urano, Y., Kikuchi, K., Hirata, Y., and Nagano, T. (2005) Highly sensitive near-infrared fluorescent probes for nitric oxide and their application to isolated organs. *J. Am. Chem. Soc. 127*, 3684–3685.

(25) Ozmen, B., and Akkaya, E. U. (2000) Infrared fluorescence sensing of submicromolar calcium: pushing the limits of photoinduced electron transfer. *Tetrahedron Lett. 41*, 9185–9188.

(26) Kiyose, K., Aizawa, S., Sasaki, E., Kojima, H., Hanaoka, K., Terai, T., Urano, Y., and Nagano, T. (2009) Molecular design strategies for near-infrared ratiometric fluorescent probes based on the unique spectral properties of aminocyanines. *Chem.—Eur. J. 15*, 9191–9200.

(27) Yamaguchi, S., and Tamao, K. (1998) Silole-containing sigma- and pi-conjugated compounds. *J. Chem. Soc., Dalton Trans.* 3693–3702.

(28) Kyushin, T., Matsuura, T., and Matsumoto, H. (2006) 2,3,4,5-Tetrakis(dimethylsilyl)thiophene: the first 2,3,4,5-tetrasilylthiophene. *Organometallics 25*, 2761–2765.

(29) Ferman, J., Kakareka, J. P., Klooster, W. T., Mullin, J. L., Quattrucci, J., Ricci, J. S., Tracy, H. J., Vining, W. J., and Wallace, A. (1999) Electrochemical and photophysical properties of a series of group-14 metalloles. *Inorg. Chem. 38*, 2464–2472.

(30) Tracy, H. J., Mullin, J. L., Klooster, W. T., Martin, J. A., Haug, J., Wallace, S., Rudloe, I., and Watts, K. (2005) Enhanced photoluminescence from group 14 metalloles in aggregated and solid solutions. *Inorg. Chem. 44*, 2003–2011.

(31) Sohn, H., Sailor, M. J., Magde, D., and Trogler, W. C. (2003) Detection of nitroaromatic explosives based on photoluminescent polymers containing metalloles. *J. Am. Chem. Soc. 125*, 3821–3830.

(32) Tamao, K., Uchida, M., Izumizawa, T., Furukawa, K., and Yamaguchi, S. (1996) Silole derivatives as efficient electron transporting materials. *J. Am. Chem. Soc. 118*, 11974–11975.

(33) Nishiyama, K., Oba, M., Takagi, H., Fujii, I., Hirayama, N., and Narisu, Horiuchi, H. (2000) Synthesis, structure, and photochemical reaction of 9,10-dihydro-9-silaanthracene derivatives carrying bulky substituents. *J. Organomet. Chem. 604*, 20–26.

(34) Fu, M., Xiao, Y., Qian, X., Zhao, D., and Xu, Y. (2008) A design concept of long-wavelength fluorescent analogs of rhodamine dyes: replacement of oxygen with silicon atom. *Chem. Commun. 15*, 1780–1782.

(35) Although several names have been given to xanthene chromophores whose oxygen atom at the 10 position is replaced by other atoms, including pyronine, rhodamine, and xanthylium dye, in this article we call them rhodamine or pyronine, depending on whether or not a benzene ring is present at the 9 position of the xanthene chromophore (*e.g.*, Si-rhodamine and Si-pyronine).

(36) Arden-Jacob, J., Frantzeskos, J., Kemnitzer, N. U., Zilles, A., and Drexhage, K. H. (2001) New fluorescent markers for the red region. *Spectrochim. Acta, Part A 57*, 2271–2283.

(37) Arunkumar, E., and Ajayaghosh, A. (2005) Proton controlled intramolecular photoinduced electron transfer (PET) in podand linked squaraine-aniline dyads. *Chem. Commun. 5*, 599–601.

(38) Ho, N. H., Weissleder, R., and Tung, C. H. (2006) Development of water-soluble far-red fluorogenic dyes for enzyme sensing. *Tetrahedron 62*, 578–585.

(39) Calitree, B., Donnelly, D. J., Holt, J. J., Gannon, M. K., Nygren, C. L., Sukumaran, D. K., Autschbach, J., and Detty, M. R. (2007) Tellurium analogues of rosamine and rhodamine dyes: synthesis, structure, ^{125}Te NMR, and heteroatom contributions to excitation energies. *Organometallics 26*, 6248–6257.

(40) Detty, M. R., Prasad, P. N., Donnelly, D. J., Ohulchanskyy, T., Gibson, S. L., and Hilf, R. (2004) Synthesis, properties, and photodynamic properties in vitro of heavy-chalcogen analogues of tetramethylrosamine. *Bioorg. Med. Chem. 12*, 2537–2544.

(41) Dijk, M. A., Kapitein, L. C., Mameren, J., Schmidt, C. F., and Peterman, E. J. (2004) Combining optical trapping and single-molecule fluorescence spectroscopy: enhanced photobleaching of fluorophores. *J. Phys. Chem. B 108*, 6479–6484.

(42) Eggeling, C., Widengren, J., Rigler, R., and Seidel, C. A. M. (1998) Photobleaching of fluorescent dyes under conditions used for single-molecule detection: evidence of two-step photolysis. *Anal. Chem. 70*, 2651–2659.

(43) Overly, C. C., Lee, K. D., Berthiaume, E., and Hollenbeck, P. J. (1995) Quantitative measurement of intraorganelle pH in the endosomal-lysosomal pathway in neurons by using ratiometric imaging with pyranine. *Proc. Natl. Acad. Sci. U.S.A. 92*, 3156–3160.

(44) Nachliel, E., Gutman, M., Kiryati, S., and Dencher, N. A. (1996) Protonation dynamics of the extracellular and cytoplasmic surface of bacteriorhodopsin in the purple membrane. *Proc. Natl. Acad. Sci. U.S.A. 93*, 10747–10752.

(45) Johnson, V. L., Walsh, L. M., and Chen, B. L. (1980) Localization of mitochondria in living cells with rhodamine 123. *Proc. Natl. Acad. Sci. U.S.A. 77*, 990–994.

(46) Vallee, B. L., and Falchuk, K. H. (1993) The biochemical basis of zinc physiology. *Physiol. Rev. 73*, 79–118.

(47) Frederickson, C. J., Koh, J. Y., and Bush, A. I. (2005) The neurobiology of zinc in health and disease. *Nat. Rev. Neurosci. 6*, 449–462.

(48) Domaille, D. W., Que, E. L., and Chang, C. J. (2008) Synthetic fluorescent sensors for studying the cell biology of metals. *Nat. Chem. Biol. 4*, 168–175.

(49) Hu, H., Bandell, M., Petrus, M. J., Zhu, M. X., and Patapoutian, A. (2009) Zinc activates damage-sensing TRPA1 ion channels. *Nat. Chem. Biol. 5*, 183–190.

(50) Tang, B., Huang, H., Xu, K., Tong, L., Yang, G., Liu, X., and An, L. (2006) Highly sensitive and selective near-infrared fluorescent probe for zinc and its application to macrophage cells. *Chem. Commun. 13*, 3609–3611.